Old Questions and New Results — Recent Advances in Superconductivity

A. Wittlin*

Institute of Physics, Polish Academy of Sciences, al. Lotników 32/46, Warsaw, Poland

Received: 30.01.2025 & Accepted: 11.03.2025

Doi: 10.12693/APhysPolA.147.370

*e-mail: wittlin@ifpan.edu.pl

The mechanism of high-temperature superconductivity remains a subject of research, although there is a fairly widespread view that it is not the classical Bardeen–Cooper–Schrieffer mechanism. One of the most active critics of the Bardeen–Cooper–Schrieffer theory is J. Hirsch, who also presents his hole superconductivity model as a theory that better describes this phenomenon. We review the current state and prospects of experimental confirmation of the hole theory of superconductivity and discuss the results of contemporary experimental and theoretical works related to issues identified as significant tests of the credibility of this theory.

topics: Bardeen–Cooper–Schrieffer (BCS) theory, pairing mechanism, superconducting gap, Meissner effect

1. Introduction

The question of the mechanism or mechanisms of superconductivity in the recently discovered families of high-temperature superconductors, as well as the question of the possibility of achieving superconductivity at room temperature, are among the most important issues in contemporary physics, also due to their potential applications. In the economy, the growing demand for better superconductors with higher critical temperatures and easier technology for producing cheap superconducting cables is stimulated by economic problems related to energy acquisition and electro-mobility. In the field of physics, the prospect of building large next-generation particle accelerators is largely dependent on the ability to construct cheap and easy-to-operate strong superconducting magnets.

Up to now, the only complete theory of superconductivity is the BCS theory of J. Bardeen, L.N. Cooper, and J.R. Schrieffer [1] (the abbreviation "BCS" comes from the founders' names). However, this theory is strongly criticized, and not only because of the limitations of proposed pairing mechanism.

In the opening sentence of their seminal 1957 paper *Theory of Superconductivity* [1], J. Bardeen, L.N. Cooper, and J.R. Schrieffer outline several key phenomena that their theory must address. These include: (i) a second-order phase transition at the critical temperature (T_c); (ii) the electronic specific heat, which varies as $\exp(-T_0/T)$, along with other evidence for an energy gap in individual particle-like excitations; (iii) the Meissner–Ochsenfeld effect, which results in the magnetic field $B = 0$; (iv) effects linked to perfect conductivity, where the electric field $E = 0$; and (v) the relationship between T_c and isotopic mass, expressed as $T_c\sqrt{M} = \text{const}$.

The BCS theory, as their work is known, became a phenomenal success as the first presentation of the microscopic mechanism of superconductivity in metals. It explained several phenomena discovered earlier and predicted many that were observed later. Together with subsequent extensions and modifications, it became an essential tool for several generations of condensed matter physicists and is described in numerous textbooks in higher education in physics [2–6]. Recently, studies in the mathematics of the BCS functional have become an active field of research in its own right [7]. The BCS theory was not seriously contested for almost half a century after its inception, although it was recognized early on that it had limited predictive power with respect to the critical temperature. This changed dramatically forty years ago with the discovery of high-temperature superconductors and, later, iron-based superconductors, which have complex crystalline structures, low-symmetry order parameters, and a variety of properties that are radically different from those of classical superconductors. At present, although we still do not fully understand the mechanism of superconductivity in these compounds, the prevailing view is that it is not based on electron–phonon interaction. Another unresolved issue is the detailed explanation of the Meissner phenomenon and, more generally, the description of certain electrodynamic phenomena in superconductors under an external magnetic field.

The experimental discovery of high-temperature superconductors in the late 1980s also led to many proposals of new, non-BCS theories, like: spin-fluctuations-related pairing [8], resonating-valence bonds [9], spin-bags pairing [10], or marginal Fermi liquid physics [11] — but none of these has gained general acceptance to date. One such theory, the hole superconductivity theory, was proposed by Jorge Eduardo Hirsch (JEH) [12–22], who, in the meantime, has also become a vocal critic of the BCS theory [23]. His model of superconductivity, developed over more than 30 years, describes the mechanism of superconductivity within the framework of the so-called *Dynamic Hubbard Model*. In this description, the formation and condensation of pairs in the superconducting phase below T_c occur due to the lowering of the kinetic energy of holes (current carriers in the metal above the critical temperature) through "decorrelation," described as a reduction in the effective mass of the carriers. The mechanism of superconductivity is purely electronic, without the involvement of phonons. In numerous works, J.E. Hirsch presents an alternative view of the physics of superconductors compared to the BCS model and, among other things, proposes experiments that, in his opinion, should determine the credibility and predictive capability of his theory.

In this brief review of the current state and prospects of experimental confirmation of the hole theory of superconductivity, we will discuss the results of contemporary experimental and theoretical works related to the issues highlighted as significant tests of the theory's credibility.

J.E. Hirsch published over a hundred scientific articles in the last 35 years [24], dedicated to criticizing the BCS theory, demonstrating, in his opinion, its numerous flaws, presenting phenomena unexplained by the theory, or thought experiments that contradict it. At least part of his criticism seems justified and therefore worthy of attention.

The BCS theory did not predict superconductivity in almost any of the new superconductors discovered since its announcement, especially in superconducting copper oxides and iron-based compounds, and, as discussed below, there are certain not well understood aspects of the Meissner effect.

More recently, JEH has attracted the global attention once again by actively participating in the scientific debate on the validity and interpretation of data in several high-profile publications concerning possible room-temperature superconductivity. There, the question of the applicability of the BCS theory has recently re-emerged as a focal point of condensed matter physics research, particularly in connection with the growing number of experimental results related to the electrical properties of hydrogen-rich compounds under high hydrostatic pressure. The perspective outlined by N. Ashcroft in 1968, which proposed the possibility of room-temperature superconductivity in high-pressure metallic hydrogen based on the mechanism described in the BCS theory [25] (and later extended to include metal hydrides [26]), has recently been revisited in the light of experimental findings. These studies claimed to have observed superconductivity at near-room temperature under extremely high hydrostatic pressure in various hydrogen-rich compounds. Some of these results have been publicly challenged, with certain findings being considered false, while others remaining the subject of scientific debate. JEH has been an active participant in this debate, both as an insightful public reviewer of experimental results and as a critical skeptic of the possibility of achieving room-temperature superconductivity through the electron–phonon interaction mechanism described by the BCS theory. He and his collaborators have critically analyzed the contested data, leading to the retraction of several of these high-profile papers and prompting investigations into possible scientific fraud committed by some of the authors [27–33]. The question of achieving or potentially achieving superconductivity in these materials at room temperature remains open [34].

In the following sections, we will discuss three selected issues of Hirsch's theory and their experimental status. We are guided by the importance that the authors of the theory place on the experimental confirmation of their theses in order to validate the model of hole superconductivity, which is significantly different from the BCS model. These are questions concerning: the source of superconducting carriers, the electric fields on the surface of the superconductor, and the details of the energy and angular momentum balance in the Meissner–Ochsenfeld effect.

JEH presents a series of experimental proposals in his works that, in his opinion, could validate the theory of hole superconductivity. His most recent published work [22] lists, among these experiments, predicted violations of the sum rule for alternating current (AC) conductivity and postulates a significant increase in the screening length in the superconducting phase. Below, we will discuss two recently conducted experiments that investigated these conjectures.

2. "Violated sum rules" or superconductivity-induced "color changes"

In early articles on the hole theory of superconductivity [35, 36], the authors, based on their calculations and the then available partial optical data for high-T_c cuprates, predicted a violation of the optical sum rule for the in-plane response in cuprates. The optical sum rule, originally formulated a century ago by F. Reiche and

W. Thomas [37], and W. Kuhn [38] and later expanded by W. Kohn [39], states that the sum of the oscillator strengths of all optical transitions equals the total number of electrons. This rule is rooted in fundamental physical principles, including charge conservation and temporal causality [40]. Together with the Kramers–Kronig transformations [41]

$$\sigma_1(\omega) = \frac{2}{\pi}\mathcal{P}\left[\int_0^{\infty} \mathrm{d}\omega' \, \frac{\omega'\sigma_2(\omega')}{\omega'^2 - \omega^2}\right],$$

$$\sigma_2(\omega) = -\frac{2}{\pi}\mathcal{P}\left[\int_0^{\infty} \mathrm{d}\omega' \, \frac{\sigma_1(\omega')}{\omega'^2 - \omega^2}\right], \tag{1}$$

where $\sigma(\omega) = \sigma_1(\omega) + \mathrm{i}\sigma_2(\omega)$ is the complex conductivity; the sum rule is a standard tool for analyzing the optical spectra of semiconductors and metals. The sum rule for the real part of the frequency-dependent conductivity σ_1 is

$$\int_0^{\infty} \mathrm{d}\omega \; \sigma_1(\omega) = \frac{\omega_p^2}{8}, \tag{2}$$

where $\omega_p = \sqrt{4\pi N e^2/m}$ is the plasma frequency. In superconductors, the sum rule, combined with the temperature evolution of the frequency-dependent complex conductivity (often represented as a superposition of Lorentz oscillators), provides insights into the charge carrier dynamics. It aids in observing carrier condensation, in analyzing the temperature dependence of the excitation gap in the superconducting condensate spectrum, and in determining the variation of penetration depth with temperature. The sum rule is particularly valuable for studying the temperature-dependent spectral weight flow near the critical temperature, which sheds light on the microscopic mechanisms of superconductivity. For classical BCS superconductors, the complex conductivity is described by the Mattis–Bardeen model [42, 43], which offers a quasi-analytical description of the spectrum. Glover and Tinkham [44] conducted the first temperature-dependent far-infrared spectroscopic measurements of classical superconductors, such as lead and tin, demonstrating the presence and width of an energy gap that appears in the far-infrared spectrum below the critical temperature. Subsequently, Tinkham and Ferrell [45] explained that the spectral weight diminished at energies below the gap 2Δ (the so-called "missing area") reappears in the conductivity spectrum as a delta peak at zero frequency. Physically, this "infinite" direct current (DC) conductivity corresponds to the absorption of energy from an electric field to supply the kinetic energy of the accelerated supercurrent. Plot of the real part of a BCS superconductor conductivity as a function of frequency for temperatures above T_c and below T_c is shown in Fig. 1. The hatched ("missing" at $T = 0$) area is numerically equal to the integral of the delta function $\delta(\omega)$, the density of the condensate d_s.

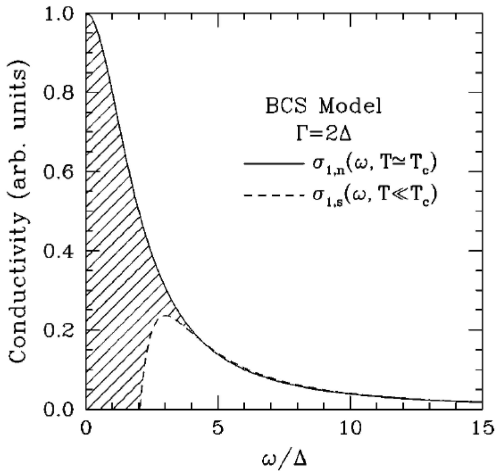

Fig. 1. The real part of the optical conductivity calculated for a BCS model for a normal-state scaterring rate of $\Gamma = 2\Delta$. The conductivity in the normal state $\sigma_1(\omega, T > T_c)$ is shown by the solid line (normalized to unity), while the conductivity in the superconducting state $\sigma_1(\omega, T < T_c)$ is shown by the dashed line. For $T \ll T_c$ the superconducting gap 2Δ is fully formed and there is no absorption below this energy. The hatched area illustrates the spectral weight that has collapsed into the superconducting $\delta(\omega)$ function at the origin. The figure is reproduced from [46].

In the BCS picture of the superconducting state, the electron density of states shifts upward in energy away from the gap region, increasing the kinetic energy of the electrons. This increase is offset by the pairing energy of Cooper pairs and the zero-point kinetic energy of phonons. The delta-function conductivity, associated with the "infinite" DC conductivity of the critical current (the superfluid density d_s), compensates for the missing spectral weight in the gap region. As the material is cooled below T_c, the normal-state spectral weight of conducting electrons gradually disappears due to the pairing of carriers. Therefore, it results in the superconducting phase spectral weight "missing area" corresponding to the condensate density, i.e.,

$$d_s = \frac{2}{\pi}\int_{0^+}^{\infty} \mathrm{d}\omega \, \Big[\sigma_{1N}(\omega) - \sigma_{1S}(\omega)\Big] = \frac{2}{\pi}\int_{0}^{0^+} \mathrm{d}\omega \; \sigma_{1S}(\omega), \tag{3}$$

where the subscript "S" is for superconducting and "N" is for normal, above T_c phase. Nevertheless, the total integrated conductivity and the Ferrell–Glover–Tinkham (FGT) sum-rule integral (2) remain unchanged. Furthermore, the temperature–energy balance of the spectral weight demonstrates that in the measured metals, microscopic phenomena relevant to superconductivity occur at energies below the gap, which is consistent with the BCS theoretical predictions. In the model of hole superconductivity, electron pairing occurs at the expense of kinetic energy, due to the weakening of electron correlations in the excitation energy range of interband transitions, i.e., a few electron volts. The authors of the hole theory of superconductivity in cuprates predicted that, contrary to the behavior of BCS superconductors, the spectral weight contributing to the superconducting condensate — the "missing area" — would originate from energies much larger than the gap, extending into the visible range of the spectrum [35, 36, 46]; this phenomenon is referred to as the "sum-rule violation" or "superconductor color change."

Early experimental results from studies of optical conductivity in cuprate superconductors did not provide a clear understanding of the optical spectra or the balance of spectral weight according to the sum rule. Hereafter we shall discuss only the a–b plane optical conductivity in cuprates, which is easier to measure and less dependent on the chemical composition of the superconductor than the out-of-plane conductivity. In particular, conflicting conclusions were drawn from data on nominally identical materials. Confirmation of the FGT sum rule was reported for underdoped or optimally doped cuprates, specifically for the in-plane conductivity of $YBa_2Cu_3O_7$ [46, 47] and underdoped $Bi_2Sr_2CaCu_2O_{8-\delta}$ [43]. The violation of the FGT was reported for the in-plane conductivity of underdoped $Bi_2Sr_2Ca_2Cu_{8-\delta}$ [48, 49], optimally doped $Bi_2Sr_2Ca_2Cu_8O_8$ [48], and optimally doped $Bi_2Sr_2Ca_2Cu_3O_{10}$ [50]. Published estimates of the condensation energy of bismuth-based superconductors (in meV per copper atom) were: 0.06–0.25 (depending on doping) [48], 0.5–1 (underdoped) [51], and 1.1 ± 0.3 (underdoped) [49]. The critical temperatures of the samples studied (crystals and thin films) were very similar, ranging from 63 to 88 K, but the scatter in the determined condensation energies was over 2000%. Possible reasons for these discrepancies, including sample quality, model-fitting-dependent procedures, and experimental inaccuracies, were discussed in [52, 53].

The complex conductivity is typically calculated from the frequency-dependent complex refractive index $\hat{N} = n(\omega) + \mathrm{i}k(\omega)$, where $n(\omega)$ is the refractive index and $k(\omega)$ is the extinction coefficient. These values are either directly obtained from experiments or calculated using the Fresnel equations based on measured (complex) transmission and/or reflectivity data. It is important to emphasize that in order to obtain the complete complex conductivity, two measured quantities from optical experiments are required — the intensity and phase of either the transmitted or reflected electromagnetic waves at each frequency. Conducting such research over a broad frequency range is challenging and often prone to errors. It typically necessitates combining various measurement techniques, different sources of electromagnetic radiation, and different types of spectrometers. The next step in data analysis usually involves carefully fitting (preferably with partially overlapping) the measured spectra to obtain as complete a picture of the complex conductivity as possible, spanning a range from low microwave frequencies to ultraviolet, while minimizing errors in the resulting sum of oscillators for the material. Recent studies by Dawson et al. [54], published in 2023, seem to have overcome earlier challenges and have enabled a precise investigation of the temperature dependence of the complex conductivity in the a–b plane of high-temperature superconductors, specifically of $DyBa_2Cu_3O_7$ [54]. Samples for these measurements were grown using the MBE (molecular beam epitaxy) technique as oriented thin films (70 nm thick and 10×10 mm^2 in size). The sample sizes were sufficiently large to allow optical measurements in the very low microwave energy range without diffraction effects. The authors of [54] measured the complex conductivity in the energy range from 0.8 meV to 1.1 eV and at temperatures ranging from 7 to 300 K. Due to the specific nature of the spectral ranges studied, three different measurement techniques were used: quasi-optical microwave measurements with a Mach–Zehnder interferometer, terahertz spectroscopy using a LaserQuantum HASSP spectrometer in the far-infrared range, and ellipsometry in the infrared range.

The results of the study [54] show that below T_c, the spectral weight transfer to the superconducting condensate is almost entirely confined to the energy range below 110 meV, accounting for 95% of the total. The remaining 5% originates from a very slightly temperature-dependent region of the spectrum between 110 and 600 meV. Above 0.6 eV, extending up to over 1 eV, the measured complex conductivity is temperature-independent. These results are consistent with previously published data, obtained using less precise methods, for $YBa_2Cu_3O_{7-\delta}$ crystals, but do not confirm other results, particularly those presented for $Bi_2Sr_2Ca_2Cu_8O_8$ family compounds, which report superconductivity-induced transfer of the spectral weight from the above 1–2 eV range.

The authors of [54] conducted and presented a very detailed analysis of possible measurement errors. In particular, independent measurements of the real and imaginary parts of the complex conductivity allowed for the comparison of the measured σ_1 with the Kramers–Kronig transform calculated from the measured σ_2, and vice versa. The comparison showed nearly perfect agreement, demonstrating the accuracy and consistency of the procedures applied.

The key result of the study, relevant to our discussion, is presented in Fig. 2, which shows the total measured spectral weight (black dots) below 0.6 eV, normalized to the spectral weight measured at T_c, as a function of temperature in units of T_c. The measurement points below T_c indicate that the total spectral weight does not change with temperature

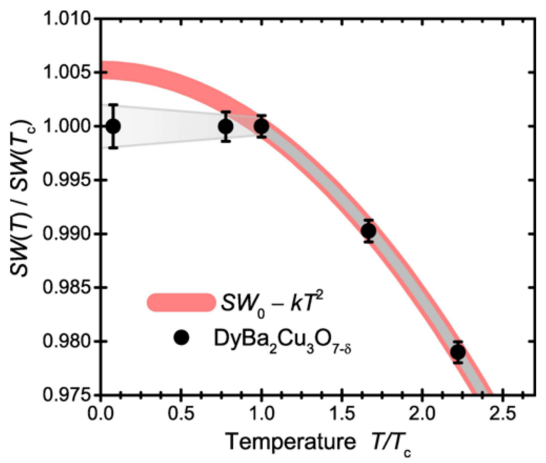

Fig. 2. The total intraband SW of the 60 u.c. thick DyBCO film as a function of reduced temperature, normalized to its value at T_c. Above T_c the quasiparticle SW follows the quadratic dependence $\mathrm{SW}(T) = \mathrm{SW}(0) - kT^2$ (red shaded line). Below T_c the total intraband SW remains constant to within the error bar. At the lowest measured temperature of 7 K this constitutes a superconductivity-induced reduction of the intraband SW of $\sim$0.5% compared to the normal state single-band value. The figure is reproduced from [54].

to within an accuracy better than 0.2%. The red parabola in Fig. 2 represents a fit to the results for $T > T_c$, based on the spectral weight's temperature dependence calculated using the nearest-neighbor interaction model within the tight-binding approximation for the layered system $\mathrm{DyBa_2Cu_3O_{7-\delta}}$.

In analyzing the confirmation of the precise fulfillment of the FGT sum rule in the studied material, the authors of [54] emphasize that "their results rule out unusual kinetic energy saving pairing mechanisms, like JEH theory [35, 36] as the prime driver of superconductivity in optimally doped RBCO cuprates."

The presented results and conclusions drawn in [54] clearly indicate the need to re-measure precisely the temperature dependence of the AC conductivity of other high-temperature superconductors from the copper group family, in particular Bi, Ta, and Hg-based and, probably, to revise the conclusions drawn from earlier works.

3. Alternative electrodynamics

One of the consequences of the superconductivity model developed by JEH is the postulation of a redistribution of the electric charge density, including electrons and holes, in the superconducting phase [21]. According to the author's model, below the critical temperature, electrons move from the bulk of the superconductor to its surface, creating a "macroscopic quantum state." This state is characterized by several features, including a non-uniform charge distribution, with a predominance of positive charges in the bulk and negative charges near the surface. This redistribution results in a decrease in the electrons' kinetic energy at the expense of an increase in their potential energy. JEH further argues that while in a non-superconducting metal, the Coulomb repulsion and screening eliminate the electric field in the bulk, in a hole-based superconductor (similar to a "giant atom"), a macroscopically non-uniform electric field distribution is possible. To better present the key postulates of his model and their potential experimental consequences, the author employs a modified version [55] of the phenomenological model of superconductor electrodynamics developed by the London brothers in the 1930s [56, 57].

The London brothers in their phenomenological description of the interaction between the electromagnetic field and a superconductor (published shortly after the discovery of the Meissner–Ochsenfeld effect [58]) discuss, among other things, the non-physical aspects of the previously proposed "Ohm's law for superconductors" [56, 59]. Henceforth, we follow the notation from [60], thus

$$\frac{\partial \boldsymbol{v}_s}{\partial t} = \frac{e}{m_e}\boldsymbol{E}, \tag{4}$$

where $\boldsymbol{v}_s$ is the velocity of the superfluid composed of carriers with effective mass m_e and charge e, and $\boldsymbol{E}$ is the electric field. The transformed equation (4), along with the London equation

$$\nabla \times \boldsymbol{J}_s = -\frac{c}{4\pi\lambda_{\mathrm{L}}^2}\boldsymbol{B}, \tag{5}$$

where λ_{L} is the London penetration depth, allows the authors to derive the symmetric wave equation for the magnetic field $\boldsymbol{B}$

$$\nabla^2 \boldsymbol{B} = \frac{1}{\lambda_{\mathrm{L}}^2}\boldsymbol{B} \tag{6}$$

and analogous equations for the electric field and current density. This leads to the following equation [55]

$$\frac{\partial \boldsymbol{J}_s}{\partial t} = \frac{c^2}{4\pi\lambda_{\mathrm{L}}^2}\left(\boldsymbol{E} + \nabla\phi\right), \tag{7}$$

where the right-hand side contains a gradient term, originally inserted, later removed, and then re-introduced by J.E. Hirsch [55]. This term allows for the presence of an electric field in the superconductor, which is necessary for the hole-based superconductivity model to describe the superconducting phase. Hirsch proposes an experiment to test the validity of the modified London equation, aiming to measure the magnitude of the non-homogeneous induced local charge density on the surface of a superconducting metal [60]. According to his model, this surface charge density should differ from the one observed in the normal state, above the critical temperature. It is illustrated in Fig. 3.

The first experimental attempt to study the potential difference in the interaction of an electric field with the surface of a superconducting metal, compared to the interaction with the same surface in the normal state, was published already by H. London in 1935 [59]. He constructed an electric condenser consisting of two parallel mercury plates, separated by an 18-micron thick mica foil, cooled to 1.8 K. Through careful and accurate measurements of the condenser's capacitance, London observed no difference between the superconducting and normal states of mercury, which could be switched on and off reproducibly with an external magnetic field. He concluded that there is no electrostatic field in the superconductor and therefore, in the proposed earlier equation

$$\frac{\partial J_s}{\partial t} = \frac{n_s e^2}{m} \left(E + \text{grad}\ \phi\right), \tag{8}$$

the term grad ϕ must be zero. However, the negative result of that experiment was interpreted by JEH [60] as unrelated to the problem of the presence of the electric potential gradient term in the equation due to the uniform electric field between the plates in London's condenser and, consequently, a shift of superfluid compensating possible changes in capacitance. In a similar way, JEH justified the failure of other, later, similar but unpublished experiments that he discussed.

A modern version of H. London's experiment, adapted to the measurement scheme proposed by JEH in [60], was recently conducted by Peronio and Giessibl [61]. Although the measurements have not provided an answer to the question of whether electric charge can accumulate in the volume of a superconductor yet, the experiment appears very interesting and may, together with other contemporary results, help to provide an answer to the question raised 90 years ago. The authors of the study investigated the effect of the superconducting state on the force between the atomic force microscopy (AFM) probe and a properly prepared surface of a thin niobium layer, whose electrical state could be simultaneously monitored using a scanning tunneling microscope (STM) probe. In their contemporary experiment, the strength of interaction corresponding to the gradient of the force between the tip and the sample is measured as the frequency deviation Δf from the natural oscillation frequency of the (unperturbed) sensor f_0, i.e.,

$$\Delta f = \frac{2f_0}{\pi k A^2} \int_{-A}^{A} \mathrm{d}z\ k_{ls}\left(z\right) \sqrt{A^2 - z^2}, \tag{9}$$

where A is the oscillation amplitude of the tip, k is the stiffness of the sensor, and k_{ls} is a position-dependent "spring constant" of the sensor–sample force. Measurements were carried out at temperatures of 2.4, 4.5, and 9.5 K, both below and above T_c.

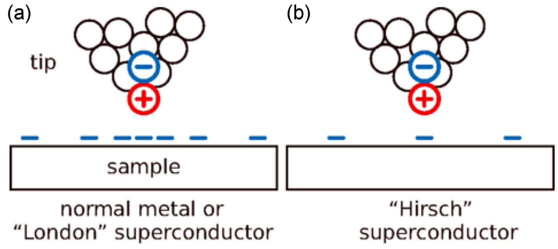

Fig. 3. The response of a superconductor to the electric field of an AFM tip apex. (a) A "London" superconductor screens an applied field like a normal metal, within the Thomas–Fermi screening length of about 0.1 nm. (b) The screening of a "Hirsch" superconductor is instead much weaker, with a characteristic length of 39 nm for niobium at zero temperature. The figure is reproduced from [61].

The results of the measurements at 9.5 and 4.4 K, shown in Fig. 4, revealed no effect on the interaction force between the probe and the surface, within the carefully estimated small measurement error. The results for 2.4 K (not shown here) are almost identical to these at 4.4 K. The limitation of the measurement, for reasons discussed below, was the relatively narrow temperature range between high temperature of 9.5 K, which is above T_c, and the lowest available temperature of 2.4 K. In this range, the density of superconducting condensate in niobium can be described by the Gorter–Casimir two-fluid model [4], which includes both the superconducting condensate phase and the "normal" phase of single-particle excitations. According to JEH, for the superconducting phase, the appropriate screening length for the electric field interaction with the probe is the London penetration depth $\lambda_{\mathrm{L}} = c/\omega_p = \sqrt{m/(\mu_0\, n\, q^2)}$, where m, n, q are the superconducting carrier mass, density, and charge, respectively. In the non-superconducting phase, the screening length is much shorter, corresponding to the Thomas–Fermi screening length $\lambda_{\mathrm{TF}} = \sqrt{\pi a_0/(4k_{\mathrm{F}})}$. In measurements, the latter will dominate due to the effective screening length, which takes both mechanisms into account, as discussed below.

Within the framework of the two-fluid model with $t = T/T_c$, the (empirical) density of the superconducting condensate is $n_s = n\,(1-t^4)$, and the density of single-electron excitations is $n_n = n - n_s$. The effective screening length at temperatures between 0 and T_c is a weighted average of λ_{L} and λ_{TF} with contributions proportional to the density of carriers [60, 62],

$$\frac{1}{\lambda_{eff}(T)} = \frac{n_s(T)}{n\,\lambda_{\mathrm{L}}^2} + \frac{n_n(T)}{n\lambda_{\mathrm{TF}}^2}. \tag{10}$$

The influence of the first term of the right side of (10) will prevail only when $n_n(T)/n < 1/(\lambda_{\mathrm{L}}^2/\lambda_{\mathrm{TF}}^2 + 1) \approx (\lambda_{\mathrm{TF}}/\lambda_{\mathrm{L}})^2$. For niobium, with $\lambda_{\mathrm{TF}} \approx 0.1$ nm and $\lambda_{\mathrm{L}} \approx 40$ nm this occurs at

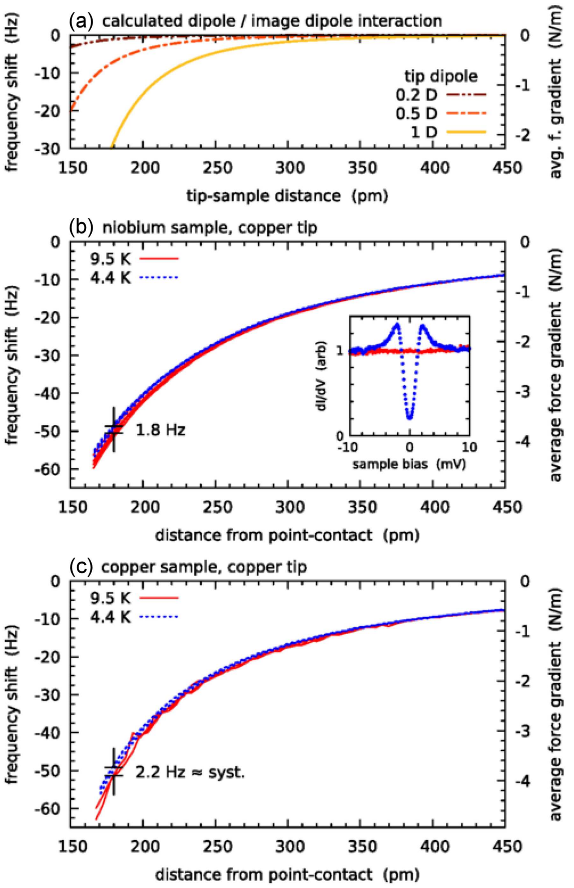

Fig. 4. (a) Frequency shift due to the dipole/image dipole interaction calculated for different tip dipoles and for the oscillation amplitude $A = 50$ pmpk used in the experiments in (b) and (c). $\Delta f(z)$ spectra at two different temperatures (b) on Nb(110) and (c) on Cu(110). Only at $T = 4.4$ K does the Nb sample superconduct, as shown by the $\mathrm{d}I/\mathrm{d}V$ spectroscopy of the superconductive gap (inset). The $\Delta f(z)$ spectra at the two temperatures are different on Nb, but this effect cannot be attributed to Hirsch superconductivity since it is observed also on Cu. These spectra are acquired at the same point on the surface, and multiple measurements are shown. The measurements in (b) were acquired in different heating–cooling cycles. The $\mathrm{d}I/\mathrm{d}V$ spectra are acquired at a tunneling set point $V = -20$ mV, $I = 200$ pA with a modulation voltage $V_m = 300$ μV$_{\mathrm{pk}}$ at $f_m = 407$ Hz. The figure is reproduced from [61].

approximately $t < 0.12$, below 1.1 K[†1]. This typically requires a ^{3}He or dilution refrigerator cooling system, which might be difficult to combine with an AFM setup. Moreover, as already mentioned in [61], the experimental difficulties associated with repeatedly warming the system above T_c and its subsequent cooling may be even more serious, expensive, and time-consuming. With mercury as the sample, perhaps a magnetic field could be used to suppress superconductivity. One could consider studying high-T_c superconductors with sufficiently large n (which may or may not be BCS superconductors), as this would make fulfilling the condition $t < 0.12$ easier, assuming that a high-quality sample surface could be prepared. Perhaps some clues regarding the further use of scanning microscopic techniques to investigate the presence of an electric field in a superconductor could also be provided by the contemporary results on Cooper pair imaging in $Bi_2Sr_2CaCu_2O_{8+x}$ in [63–65]. The authors of these papers used a scanning tunneling microscope and Josephson tunneling, achieving a resolution of about 1 nm at temperatures below 50 mK, imaging, among other things, individual Zn atoms on the surface of the superconductor and other nanoscale superconductivity-related phenomena.

[†1]This estimate assumes that the two-fluid model equation of the temperature dependence of the condensate density is correct, but see also the comment by M. Tinkham in [4] on page 104.

4. Thermodynamic phenomena

An important physical phenomenon that, according to JEH, the BCS theory fails to accurately describe is the Meissner–Ochsenfeld effect. First observed in 1933 by W. Meissner and R. Ochsenfeld, this effect demonstrated the "expulsion" of magnetic flux from the interior of lead or tin samples cooled to the superconducting state. It is widely regarded as the most significant manifestation of the magnetic properties of superconductors and a demonstration of the "true nature of the superconducting state" [66], particularly for Type I superconductors.

The theses of JEH regarding the inapplicability of the BCS model to describe the Meissner effect, which do not align with the mainstream narrative in contemporary physics, are presented here in order to demonstrate the types of problems encountered in research within the field of superconductivity, especially — but not limited to — high-temperature superconductivity. The JEH's current polemics with one of the influential scientific journals are included in the document [67] posted on his website.

The first phenomenological description of this phenomenon was provided by F. London and H. London [56]. They proposed that in a weak static magnetic field $B(x)$, the current density in a superconductor could be expressed as $\boldsymbol{J} = -\Lambda \boldsymbol{A}$, where $\boldsymbol{A}$ is the magnetic vector potential. The resulting wave equation has a physically admissible solution $B(x) = B_0 \exp(-x/\Lambda(T))$, where $\Lambda(T)$ is the temperature-dependent London penetration depth. The Londons' solution indicates that an external magnetic field applied to the superconductor is screened (or "expelled") by the magnetic field generated by a current flowing in a thin layer near the superconductor's surface. This result was later derived within the microscopic framework of the BCS theory [1].

In the BCS model, the Meissner–Ochsenfeld effect is reversible [4]; when samples are reheated above the critical temperature T_c, the screening current vanishes and the magnetic field penetrates the superconductor's volume. Moreover, as demonstrated by precise magnetic and calorimetric measurements conducted under near-equilibrium conditions, the change in the magnetic state of the superconductor represents a reversible phase transition without any accompanying irreversible generation of Joule heat [68] (and references herein). However, JEH emphasizes perceived shortcomings in the BCS model's description of the Meissner effect, pointing to possible energy dissipation during non-equilibrium processes associated with the transition between non-superconducting and superconducting phases, and vice versa.

JEH's analysis focuses on two key phenomena. The first concerns the angular momentum of a cylindrical Type I superconducting sample suspended along its axis, which depends on the sequence of processes, such as cooling below T_c, heating above T_c, and switching on or off the external magnetic field. The second phenomenon involves the dynamics and motion of electric charges within the sample, linked to the formation and destruction of Cooper pairs during these processes. The geometry of the described processes is illustrated in Fig. 5. J.E. Hirsch identifies three scenarios:

i. Cooling in the absence of an external magnetic field ($T < T_c$). In this case, an initially stationary superconducting sample is subjected to an increasing external magnetic field from $B = 0$ to $B_{\max} < B_c$, where B_c is the critical field. This situation essentially corresponds to that of an ideal diamagnetic metal with zero resistance. The induced screening current, generated by the varying magnetic field, produces a magnetic moment that causes the sample to rotate (gyromagnetic effect). Both the energy conservation and the angular momentum conservation are satisfied [65].

ii. Heating above T_c in an external magnetic field. A superconducting sample in an external magnetic field is heated above its critical temperature.

iii. Cooling below T_c in an external magnetic field. A normal-state sample in an external magnetic field at a temperature above T_c is cooled below its critical temperature.

In the second scenario, the non-equilibrium current of electrons from dissociating Cooper pairs in a varying magnetic field must transfer the excess momentum to the lattice. In the third, correlating electrons joining into Cooper pairs must

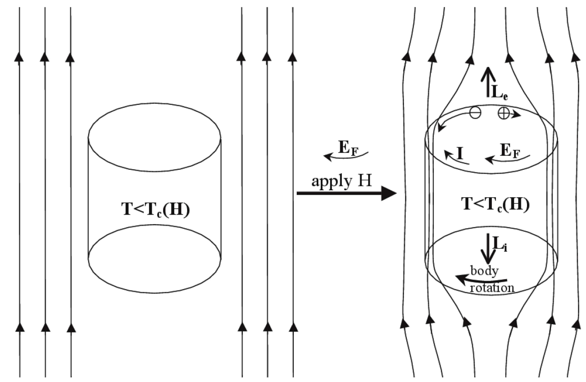

Fig. 5. A magnetic field is applied to a superconductor at rest. A Faraday electric field E_{F} is generated in the clockwise direction, opposing the change in magnetic flux. E_{F} pushes positive ions (electrons) in clockwise (counterclockwise) direction. The body acquires angular momentum L_i antiparallel to the applied magnetic field and the supercurrent acquires angular momentum $L_e = -L_i$ parallel to the magnetic field. This figure is a reproduction of Fig. 2 from [69].

acquire the momentum necessary to form a condensate. According to JEH[†2] [67, 68, 70], these non-superconducting electrons interact with their surroundings through at least partially inelastic scattering processes, which results in the generation of Joule heat, thus undermining the reversible nature of the phase transition.

The dynamics of the transition to the Meissner phase have been discussed earlier, for instance, by W.H. Cherry and J.I. Gittleman [71]. Recently, A. Schilling [72] proposed the potential compensatory effect of magnetocaloric cooling, which could result in a net-zero heat balance during the phase transition of the condensate. In Schilling's model, the magnetocaloric effect fully offsets the Joule heat, maintaining thermodynamic equilibrium and reversibility during the Meissner phase transition. However, Schilling notes that the dissipation and magnetocaloric processes in a superconductor have different spatial distributions. This suggests that, under certain material configurations and experimental conditions, it may be possible to measure temperature gradients associated with the magnetocaloric effect. These gradients, as calculated by Schilling, are expected to be small — on the order of microkelvins just below T_c — making them difficult to measure. Furthermore, various experimental constraints, such as sample geometry and homogeneity, may present additional challenges in observing the proposed effect.

[†2] J.E. Hirsch published over 40 articles discussing the Meissner effect between 2001 and 2024. The list of articles is available at author's site [70].

5. Conclusions

Of the three topics discussed regarding the experimental verification of the hole model of superconductivity, only the one related to the behavior of the sum rules in the dielectric function spectrum of high-temperature superconductors has yielded a concrete result. This result does not confirm the hypothesis of the model, but it highlights the need for re-evaluation of earlier findings obtained using less accurate methods and perhaps even with lower-quality samples produced by previous synthesis techniques. This progress was largely made possible by the experience gained from numerous earlier studies on superconducting spectroscopy and by advancements in the technology of growing high-quality, well-characterized materials.

Furthermore, the aim of this work was to better understand the mechanism of superconductivity, independent of the BCS model. The hypothesis by J.E. Hirsch regarding the accumulation of electric charges in classical superconductors was not confirmed, but the result does not conclusively refute it. The estimates obtained in the work [61] suggest potential difficulties in measuring the effect predicted by J.E. Hirsch, which would require sophisticated equipment and highly sensitive measurements at subkelvin temperatures. A similar challenge may apply to the third issue. However, the questions raised by J.E. Hirsch may serve as a stimulus for further development of research techniques and continued expansion of the sensitivity limits in measurements testing the thermodynamic and electrodynamic properties of superconductors. In other words, paraphrasing a quote often attributed to M. Planck: "Only experiment is the source of knowledge."

References

[1] J. Bardeen, L.N. Cooper, J.R. Schieffer, *Phys. Rev.* **108**, 1175 (1957).

[2] R.P. Feynman, R.B. Leighton, M.L. Sands, *The Feynman Lectures on Physics*, Vol. III: *Quantum Mechanics*, Addison-Wesley Publishing Company, Reading (MA) 1965.

[3] P.G. de Gennes, *Superconductivity of Metals and Alloys*, Benjamin 1966.

[4] M. Tinkham, *Introduction to Superconductivity*, 2nd ed., McGraw-Hill, New York 1996, Ch. 3.

[5] G.D. Mahan, *Many-Particle Physics*, 3rd ed. Kluwer Academic/Plenum Publishers, New York 2000, Ch. 10.

[6] S. Weinberg, *The Quantum Theory of Fields*, Vol. II, Cambridge University Press, Cambridge 1966, Ch. 21.6.

[7] C. Hainzl, R. Seiringer, *J. Math. Phys.* **57**, 021101 (2016).

[8] P.W. Anderson, *Science* **235**, 1196 (1987).

[9] V.J. Emery, *Phys. Rev. Lett.* **58**, 2794 (1987).

[10] J.R. Schrieffer, X.-G. Wen, S.-C. Zhang, *Phys. Rev. Lett.* **60**, 944 (1988).

[11] C.M. Varma, P.B. Littlewood, S. Schmitt-Rink, E. Abrahams, A.E. Ruckenstein, *Phys. Rev. Lett.* **63**, 1996 (1989); Erratum: *Phys. Rev. Lett.* **64**, 497 (1990).

[12] J.E. Hirsch, *Phys. Lett. A* **134**, 451 (1989).

[13] J.E. Hirsch, *Phys. Rev. B* **62**, 14487 (2000).

[14] J.E. Hirsch, *Phys. Rev. B* **62**, 14498 (2000).

[15] J.E. Hirsch, *Phys. Rev. B* **65**, 184502 (2002).

[16] J.E. Hirsch, *Phys. Rev. B* **68**, 012510 (2003).

[17] J.E. Hirsch, *Phys. Rev. B* **71**, 104522 (2005).

[18] J.E. Hirsch, *Int. J. Mod. Phys. B* **23**, 3035 (2009).

[19] J.E. Hirsch, *Int. J. Mod. Phys. B* **24**, 3627 (2010).

[20] J.E. Hirsch, *Phys. Rev. B* **87**, 184506 (2013).

[21] J.E. Hirsch, *Superconductivity Begins With H: Both Properly Understood, and Misunderstood: Superconductivity Basics Rethought*, World Scientific, Singapore 2020.

[22] J.E. Hirsch, *Hole Superconductivity* (Lecture Notes of the Autumn School on Correlated Electrons 2024, Correlations and Phase Transitions, Chpt. 7, edited by E. Pavarini, E. Koc), 2024 (preprint).

[23] J.E. Hirsch, *Phys. Scr.* **80**, 035702 (2009).

[24] J.E. Hirsch, Complete list of articles (available Apr. 2025).

[25] N.W. Ashcroft, *Phys. Rev. Lett.* **21**, 1748 (1968).

[26] N.W. Ashcroft, *Phys. Rev. Lett.* **92**, 187002 (2004).

[27] E. Snider, N. Dasenbrock-Gammon, R. McBride, M. Debessai, H. Vindana, K. Vencatasamy, K.V. Lawler, A. Salamat, R.P. Dias, *Nature* **586**, 373 (2020).

[28] D. van der Marel, J.E. Hirsch, *Int. J. Mod. Phys. B* **37**, 2375001 (2023).

[29] J. Hirsch, *Natl. Sci. Rev.* **11**, nwad174 (2024).

[30] J.E. Hirsch, *J. Supercond. Nov. Magn.* **37**, 1783 (2024).

[31] F. Capitani, B. Langerome, J.-B. Brubach, P. Roy, A. Drozdov, M.I. Eremets, E.J. Nicol, J.P. Carbotte, T. Timusk, *Nat. Phys.* **13**, 859 (2017).

[32] J.E. Hirsch, F. Marsiglio, *Nat. Phys.* **18**, 1033 (2022).

[33] P. Roy, J.-B. Brubach, F. Capitani, B. Langerome, A. Drozdov, M.I. Eremets, E.J. Nicol, T. Timusk, *Nat. Phys.* **18**, 1036 (2022).

[34] G.S. Boebinger, A.V. Chubukov, I.R. Fisher et al., *Nat. Rev. Phys.* **7**, 2 (2025).

[35] J.E. Hirsch, *Physica C* **199**, 305 (1992).

[36] J. Hirsch, F. Marsiglio, *Phys. Rev. B* **62**, 15131 (2000).

[37] F. Reiche, W. Thomas, *Naturwissenschaften* **13**, 627 (1925) (in German).

[38] W. Kuhn, *Z. Phys.* **33**, 408 (1925) (in German).

[39] W. Kohn, *Phys. Rev.* **133**, A171 (1964).

[40] R. Resta, *J. Phys. Condens. Matter* **30**, 414001 (2018).

[41] M. Dressler, G. Gruener, *Electrodynamics of Solids: Optical Properties of Electrons in Matter*, Cambridge University Press, Cambridge 2002.

[42] D.C. Mattis, J. Bardeen, *Phys. Rev.* **111**, 412 (1958).

[43] W. Zimmermann, E.H. Brandt, M. Bauer, E. Seider, L. Genzel, *Physica C* **183**, 99 (1991).

[44] R.E. Glover, M. Tinkham, *Phys. Rev.* **108**, 243 (1957).

[45] M. Tinkham, R.A. Ferrell, *Phys. Rev. Lett.* **2**, 331 (1959).

[46] C.C. Homes, S.V. Dordevic, D.A. Boon, R. Liang, W.N. Hardy, *Phys. Rev. B* **69**, 024514 (2004).

[47] A.V. Boris, N.N. Kovaleva, O.V. Dolgov, T. Holden, C.T. Lin, B. Keimer, C. Bernhard, *Science* **304**, 708 (2004).

[48] H.J.A. Molegraaf, C. Presura, D. van der Marel, P.H. Kes, M. Li, *Science* **295**, 2239 (2002).

[49] A.F. Santander-Syro, R.P.S.M. Lobo, N. Bontemps, Z. Konstantinovic, Z.Z. Li, H. Raffy, *Europhys. Lett.* **62**, 568 (2003).

[50] F. Carbone, A.B. Kuzmenko, H.J.A. Molegraaf, E. van Heumen, E. Giannini, D. van der Marel, *Phys. Rev. B* **74**, 024502 (2006).

[51] A.F. Santander-Syro, R.P.S.M. Lobo, N. Bontemps, W. Lopera, D. Giratá, Z. Konstantinovic, Z.Z. Li, H. Raffy, *Phys. Rev. B* **70**, 134504 (2004).

[52] A.B. Kuzmienko, H.J.A. Molegraaf, F. Carbone, D. van der Marel, *Phys. Rev. B* **72**, 144503 (2005).

[53] D.N. Basov, T. Timusk, *Rev. Mod. Phys.* **77**, 721 (2005).

[54] R.D. Dawson, X. Shi, K.S. Rabinovich, D. Putzky, Y.-L. Mathis, G. Christiani, G. Logvenov, B. Keimer, A.V. Boris, *Phys. Rev. B* **108**, 104501 (2023).

[55] J.E. Hirsch, *Phys. Rev. B* **69**, 214515 (2004).

[56] F. London, H. London, *Proc. R. Soc. Lond. A* **149**, 71 (1935).

[57] F. London, H. London, *Physica* **2**, 341 (1935) (in German).

[58] W. Meißner, R. Ochsenfeld, *Naturwissenschaften* **21**, 787 (1933) (in German).

[59] H. London, *Proc. R. Soc. Lond. A* **155**, 102 (1935).

[60] J.E. Hirsch, *Physica C* **508**, 21 (2015).

[61] A. Peronio, F.J. Giessibl, *Phys. Rev. B* **94**, 094503 (2016).

[62] J.E. Hirsch, *Physica C* **478**, 42 (2012).

[63] M. Hamidian, S. Edkins, S. Joo et al., *Nature* **532**, 343 (2016).

[64] Z. Du, H. Li, S.H. Joo, E.P. Donoway, J. Lee, J.C.S. Davis, G. Gu, P.D. Johnson, K. Fujita, *Nature* **580**, 65 (2020).

[65] S.M. O'Mahony, W. Ren, W. Chen, Y.X. Chong, X. Liu, H. Eisaki, S. Uchida, M.H. Hamidian, J.C.S. Davis, *Proc. Natl. Acad. Sci. U.S.A.* **119**, e2207449119 (2022).

[66] A.L. Fetter, J.D. Walecka, *Quantum Theory of Many Particle Systems*, McGraw-Hill, New York 1971.

[67] J.E. Hirsch, *Int. J. Mod. Phys. B* **34**, 2050175 (2020).

[68] J.E. Hirsch, *Phys. Rev. B* **95**, 014503 (2017).

[69] J.E. Hirsch, *Acta Phys. Pol. A* **133**, 350 (2018).

[70] J.E. Hirsch, List of articles discussing the Meissner effect (available Apr. 2025).

[71] W.H. Cherry, J.I. Gittleman, *Solid-State Electron.* **1**, 287 (1960).

[72] A. Schilling, arXiv:2407.08677, 2024.